Instability of counterpropagating beams in a two-level-atom medium

I. Bar-Joseph
AT&T Bell Laboratories, Holmdel, New Jersey 07733

Y. Silberberg
Bell Communications Research, Red Bank, New Jersey 07701
(Received 23 January 1987)

Self-oscillations are predicted for a simple nonlinear optical system consisting of two counterpropagating waves in a two-level medium. Oscillations at frequencies of T_1^{-1} and the Rabi frequency are expected for certain limits of system parameters. The physical origin of these instabilities is traced to parametric amplification in the medium. The possibility of experimental verification is discussed.

I. INTRODUCTION

Nonlinear optical systems were shown to exhibit temporal instabilities, which appear as periodic or chaotic intensity oscillations. The research has been focused on systems which include external feedback, and in particular, lasers[1] and bistable resonators.[2] The external feedback plays a crucial role in the generation of instabilities in these systems.

In previous works we have shown that instabilities can also occur when there is no external feedback,[3,4] and are therefore fundamental in nonlinear optics. We have studied the interaction of two continuous-wave counterpropagating beams in a nonlinear Kerr medium. This interaction is very common in nonlinear optics experiments, and in fact, in any interfering beam experiment there is a component of counterpropagation. We have found that such an interaction leads to a variety of time-dependent phenomena, provided that the material has a finite response time. In particular, two counterpropagating beams may undergo self-oscillations beyond a certain threshold intensity. As the intensity is increased the oscillations go, through a series of bifurcations, into a chaotic state. We have also shown that these self-oscillations can be fully explained as parametric oscillations in a distributed feedback structure formed by the phase grating in the medium.[4] We have been able to identify the various oscillation frequencies with the modes of the distributed feedback resonator and to explain their behavior as a function of the medium length and response time. Our analysis, which treated the case of a single polarization, was recently extended to include vector field interaction.[5]

The interaction of two counterpropagating beams was extensively studied in laser instabilities.[6,7] It was shown that the grating formed by the two counterpropagating beams increases the coupling between the two modes and generates instabilities. It is interesting, therefore, to study this interaction in a passive medium, with no external feedback, where other sources of instability are eliminated.

In this paper we wish to investigate the interaction of counterpropagating beams in a two-level medium (TLM). Since a TLM can be approximated (at low intensities far from resonance) by a Kerr medium, we may expect similar instabilities to appear. Resonant and coherent effects may lead to a much more complex and rich behavior in this system. However, the main motivation for this study is the possible definition of conditions for the experimental observation of some of these effects.

It is important to note that since the internal feedback arises from the interference between the two beams, the calculations are performed *without* the mean-field approximation. The analysis of the interaction in a TLM, however, is by far more complicated compared with that of a Kerr medium.

(i) The phenomenological single Debye equation, which describes the relaxation of the nonlinear index of refraction of the Kerr medium, is replaced in the TLM by three Bloch equations.

(ii) The spatial modulation of the polarization is purely sinusoidal in a Kerr medium, while saturation causes a distortion of the sinusoidal pattern and generation of higher Fourier terms in a TLM.

(iii) The number of free parameters is greater in a TLM.

Surprisingly, the TLM model can be solved analytically with only minor approximations.

We shall investigate the interaction of two equal-intensity beams in a homogeneously broadened two-level medium. In Sec. II we formulate the problem and find the steady-state solutions. In Sec. III we describe the linear stability analysis and in Sec. IV we explain several unstable solutions. Finally, in Sec. V we try to explain the physical origin of some of the instabilities and relate them to other phenomena observed in TLM. We also comment on the possibility of experimental observations.

II. STEADY-STATE SOLUTIONS

We consider two counterpropagating plane waves interacting in a TLM, as shown in Fig. 1(a). Our treatment will trivially hold for the geometry of Fig. 1(b), by replacing z by $z/\cos\theta$. The forward and backward propagating fields are given by

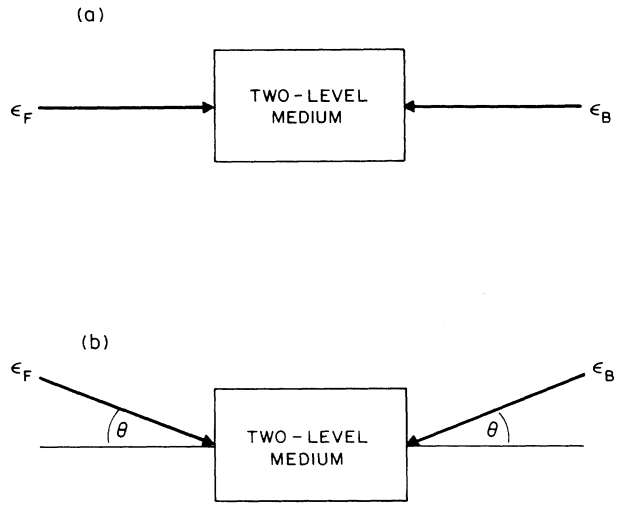

FIG. 1. Geometries for interaction. (a) Two counterpropagating beams. (b) Two interfering beams.

$$E_F(z,t)=\tfrac{1}{2}\varepsilon_F(z,t)\exp[i(\omega t-k_0 z)]+\text{c.c.}\ ,$$
$$E_B(z,t)=\tfrac{1}{2}\varepsilon_B(z,t)\exp[i(\omega t+k_0 z)]+\text{c.c}\ . \tag{1}$$

The TLM is characterized by longitudinal and transversal relaxation times T_1 and T_2, respectively. The small-signal absorption at the line center frequency ω_0 is α_0, and μ_{ab} is the atomic matrix element. The Bloch equations for the polarization S and the inversion D, induced by an electromagnetic field $E=E_F+E_B=\frac{1}{2}\varepsilon(z,t)\exp(i\omega t)+\text{c.c}$ are then[8]

$$\frac{\partial S}{\partial t}=-\frac{(1-i\delta)}{T_2}S+i\kappa\varepsilon D\ ,$$
$$\frac{\partial D}{\partial t}=-\frac{D+1}{T_1}+\frac{i}{2}\kappa(\varepsilon^* S-\varepsilon S^*)\ , \tag{2}$$

where $\kappa=2h\mu_{ab}$, $\delta=(\omega-\omega_0)T_2$, and it is assumed that in the absence of an external field the atoms are at ground state. It is clear from Eqs. (2) that both S and D would be spatially modulated by the standing-wave intensity pattern. Moreover, we can anticipate that due to saturation this modulation is not sinusoidal.

First, we find steady-state solutions for Eqs. (2). We then substitute the steady-state polarizations in Maxwell equation to get the steady-state fields. Consequently, we obtain the self-consistent values for the polarization and the inversion. This problem was previously treated by Charmichael in relation to a Fabry-Perot resonator.[9]

Setting the time derivatives in Eqs. (2) to zero, we get

$$D_{\text{SS}}=-\left[1+\frac{T_1T_2\kappa^2\varepsilon\varepsilon^*}{1+\delta^2}\right]^{-1}\ ,$$
$$S_{\text{SS}}=\frac{i\kappa T_2}{1-i\delta}\varepsilon D_{\text{SS}}\ . \tag{3}$$

From Eq. (1) it follows that

$$\varepsilon\varepsilon^*=\varepsilon_F\varepsilon_F^*+\varepsilon_B\varepsilon_B^*+\varepsilon_F\varepsilon_B^*\exp(-2ik_0z)+\text{c.c.} \tag{4}$$

We therefore expand D_{SS} in a Fourier series as

$$D_{\text{SS}}=\sum_{n=0}^{\infty}D_n(z)\cos(2nk_0z)\ , \tag{5}$$

where D_n is given by

$$D_n=\frac{1}{L}\int_0^L D_{\text{SS}}\cos(2nk_0z)dz\ . \tag{6}$$

Performing the integration of Eq. (6) we get the coefficients of the series

$$D_0=-[1+2(I_F+I_B)+(I_F-I_B)^2]^{-1/2}\ ,$$
$$D_1=\frac{I_s}{2\varepsilon_F\varepsilon_B}[(1+I_F+I_B)D_0+1]\ , \tag{7}$$
$$D_n=\frac{1}{D_0}\left[\frac{D_1}{D_0}\right]^n,\quad n=2,3,\ldots\ ,$$

where $I_F=|\varepsilon_F|^2/I_s$, $I_B=|\varepsilon_B|^2/I_s$, and $I_s=(1+\delta^2)/(\kappa^2T_1T_2)$ is the saturation intensity.

Let us define now forward and backward steady-state polarizations S_F and S_B, respectively, and expand them also in Fourier series as

$$S_F=\sum_{n=0}^{\infty}S_{F,n}(z)\exp[-i(2n+1)k_0z]\ ,$$
$$S_B=\sum_{n=0}^{\infty}S_{B,n}(z)\exp[+i(2n+1)k_0z]\ . \tag{8}$$

Substituting Eqs. (5) and (8) into Eqs. (3) yields

$$S_{F,n}=\frac{i\kappa T_2}{1-i\delta}(\varepsilon_F D_n+\varepsilon_B D_{n+1})\ ,$$
$$S_{B,n}=\frac{i\kappa T_2}{1-i\delta}(\varepsilon_B D_n^*+\varepsilon_F D_{n+1}^*)\ . \tag{9}$$

We now proceed to solve Maxwell equations, using the slowly varying amplitude approximation. Since only the first Fourier term of the polarization is phase matched these equations acquire the form

$$\frac{1}{c}\frac{\partial\varepsilon_F}{\partial t}+\frac{\partial\varepsilon_F}{\partial z}=-i\alpha_0S_{F,0}\ ,$$
$$\frac{1}{c}\frac{\partial\varepsilon_B}{\partial t}-\frac{\partial\varepsilon_B}{\partial z}=-i\alpha_0S_{B,0}\ . \tag{10}$$

By substituting Eqs. (7) into Eqs. (9) and then into (10), and setting the time derivatives to zero, we get equations for the steady-state fields. These two complex equations can be separated into four real equations for the intensities $I_{F,B}$ and phases $\Phi_{F,B}$:

$$\frac{dI_F}{dz}=-\frac{\alpha_0}{2(1+\delta^2)}\left[1-\frac{1+I_B-I_F}{[1+2(I_B+I_F)+(I_F-I_B)^2]^{1/2}}\right],$$
$$\frac{dI_B}{dz}=+\frac{\alpha_0}{2(1+\delta^2)}\left[1-\frac{1+I_F-I_B}{[1+2(I_B+I_F)+(I_F-I_B)^2}]^{1/2}\right], \tag{11}$$

$$\frac{d\Phi_F}{dz}=-\frac{1}{2I_F}\frac{\alpha_0\delta}{(1+\delta^2)}\times\left[1-\frac{1+I_B-I_F}{[1+2(I_B+I_F)+(I_F-I_B)^2]^{1/2}}\right],$$
$$\frac{d\Phi_B}{dz}=+\frac{1}{2I_B}\frac{\alpha_0\delta}{(1+\delta^2)}\times\left[1-\frac{1+I_F-I_B}{[1+2(I_B+I_F)+(I_F-I_B)^2]^{1/2}}\right].$$

If we limit ourselves to the case of very large detuning, $\delta\gg1$, and small absorption, $\alpha_0 L/\delta^2\ll1$, we can assume that the two beams are not depleted, i.e., $dI_F/dz=dI_B/dz=0$, and we can consider only the phase changes as the beams propagate along the medium. Taking the two intensities to be equal we get

$$\frac{d\Phi_F}{dz}=-\frac{\alpha_0\delta}{1+\delta^2}\frac{1}{2I}\left[1-\frac{1}{\sqrt{1+4I}}\right]\equiv-\theta,$$
$$\frac{d\Phi_B}{dz}=+\frac{\alpha_0\delta}{1+\delta^2}\frac{1}{2I}\left[1-\frac{1}{\sqrt{1+4I}}\right]\equiv+\theta, \tag{12}$$

where $I=I_F=I_B$. The steady-state field is then

$$\varepsilon_{SS}=\sqrt{I}\exp[-i(k_0+\theta)z]+\sqrt{I}\exp[+i(k_0+\theta)z], \tag{13}$$

and the self-consistent values S_{SS} and D_{SS} are given by substituting Eq. (13) into Eqs. (3).

III. LINEAR STABILITY ANALYSIS

We proceed by performing a linear stability analysis in order to determine the occurrence of a transition from stable output intensity to an unstable output intensity, namely, self-oscillations. We add small perturbations to the steady-state values ε_{SS}, D_{SS}, and S_{SS}, and take their time dependence to be $\exp(\lambda t)$. The real part of λ is the growth rate of the perturbation, while $\mathrm{Im}(\lambda)$ is its oscillation frequency Ω near the instability threshold. We note that a field oscillating at $\omega+\Omega$ may interact with the strong field at ω to generate a field at $\omega-\Omega$. We therefore write the perturbations as a sum of terms oscillating at $\pm\Omega$ and denote their amplitudes with $+$ and $-$, respectively,

$$\varepsilon(z,t)=\varepsilon_{SS}+\varepsilon_+\exp(\lambda t)+\varepsilon_-\exp(\lambda^* t),$$
$$D(z,t)=D_{SS}+d_+\exp(\lambda t)+d_-\exp(\lambda^* t), \tag{14}$$
$$S(z,t)=S_{SS}+s_+\exp(\lambda t)+s_-\exp(\lambda^* t).$$

Substituting Eqs. (14) into Eqs. (2) and retaining only first-order terms we get a set of linear algebraic equations for the perturbations, from which d_+, d_-, s_+, and s_- can be determined. The explicit expressions are given in the Appendix. Before substituting the polarization into Maxwell equation, we should note that both ε_+, the field oscillating at $\omega+\Omega$, and ε_-, the field oscillating at $\omega-\Omega$, are composed of forward and backward propagating waves. We therefore redefine the fields ε_+ and ε_- by

$$\varepsilon_+(z)=F_1(z)\exp(-ikz)+F_2(z)\exp(+ikz),$$
$$\varepsilon_-(z)=F_3^*(z)\exp(-ikz)+F_4^*(z)\exp(+ikz), \tag{15}$$

where $k=k_0+\theta$. From Eqs. (10) we get a set of linear differential equations for the F_i's,

$$\frac{dF_1}{dz}=-i\alpha_0 S_+(k)-\left[\frac{\lambda}{c}-i\theta\right]F_1,$$
$$\frac{dF_2}{dz}=+i\alpha_0 S_+(k)+\left[\frac{\lambda}{c}-i\theta\right]F_2,$$
$$\frac{dF_3}{dz}=+i\alpha_0 S^*_-(k)-\left[\frac{\lambda}{c}+i\theta\right]F_3, \tag{16}$$
$$\frac{dF_4}{dz}=-i\alpha_0 S^*_-(k)+\left[\frac{\lambda}{c}+i\theta\right]F_4,$$

where $S_\pm(k)$ are the phase-matched polarizations obtained by Fourier transform of $s_\pm$. We therefore can write Eq. (16) in a matrix form

$$\frac{d}{dz}\mathbf{F}=\mathbf{M}_1\mathbf{F}, \tag{17}$$

where $\mathbf{F}=(F_1,F_2,F_3,F_4)$. The elements of the matrix $\mathbf{M}_1$ represent phase-matched four-wave-mixing interactions which couple each F_i to the others. We shall discuss the phase matching of these interactions later. Equation (17) simplifies by defining $\mathbf{G}=(F_1+F_2,\ F_3+F_4,\ F_1-F_2,\ F_3-F_4)$ and we get

$$\frac{d}{dz}\mathbf{G}=\mathbf{M}_2\mathbf{G}, \tag{18}$$

and the matrix elements of $\mathbf{M}_2$ are given in the Appendix.

The general form of the solution of Eq. (18) is

$$\mathbf{g}(z)=\sum_{i=1}^{4}C_i\mathbf{g}_i(z)\exp(\sigma_i z), \tag{19}$$

where the $\mathbf{g}_i$'s and the σ_i's are the eigenvectors and eigenvalues of the matrix $\mathbf{M}_2$, and the C_i's are coefficients to be determined by the boundary conditions. These boundary conditions are

$$F_1(0)=F_3(0)=0,$$
$$F_2(L)=F_4(L)=0, \tag{20}$$

namely, the perturbation fields are zero at the inputs. A set of homogeneous equations for the C_i's is easily obtained by substituting Eqs. (19) into Eqs. (20), and the solutions are non-zero only if this set has a vanishing determinant.

The requirement for a vanishing determinant yields the characteristic equation. It is a complex equation which

can be used to find the unknown complex parameter λ as a function of all known system parameters. A solution with $\mathrm{Re}(\lambda)>0$ describes a growing perturbation [see Eq. (14)], i.e., an instability. Alternatively, we may find the threshold of instability by setting $\mathrm{Re}(\lambda)=0$. This condition describes a transition from a stable $[\mathrm{Re}(\lambda)<0]$ to an unstable $[\mathrm{Re}(\lambda)<0]$ solution.

IV. UNSTABLE SOLUTIONS

To study the detailed behavior of the system at the instability threshold we solved the characteristic equation setting $\mathrm{Re}(\lambda)=0$. It is a complex transcendental equation with two unknowns, the threshold intensity I_{th} and the oscillation frequency Ω. It was solved using a standard computer program for root finding. Note that there are four free parameters to this problem: the detuning δ, the small-signal absorption $\alpha_0 L$, the ratio between the two relaxation times T_2/T_1, and the transit time $t_r=L/C$. Typically, for each choice of parameters, there are many roots that solve the equation. We choose the ones with the lowest I_{th}, as these are the solutions which describe the instability threshold. In the following we consider the solutions at two limits; one of pure radiative broadening, i.e., $T_2=2T_1$, and one of rapid collisional dephasing, i.e., $T_2 \ll T_1$. We choose $\delta=100$ and $\alpha_0 L/\delta^2 \ll 1$, in order to be consistent with our assumption of undepleted fields.

Figure 2 depicts the solutions at the limit of pure radiative broadening, as a function of the transit time t_r. The threshold intensity is expressed in units of the saturation intensity I_s, the transit time in units of T_2, and the oscillation frequency in units of T_2^{-1}. The line in Fig. 2(a) describes the threshold intensity for the onset of oscillations. At lower light intensities the interaction is stable, i.e., the output intensities do not change in time. As the intensity is increased above this threshold line, the system becomes unstable, and the output waves exhibit spontaneous intensity oscillations. The threshold intensity is of the order of the saturation intensity, and as one might expect, is inversely proportional to the interaction lengths. Solutions, however, are found only in a limited length range, where $t_r \ll T_2$. The frequency of these oscillations is given at Fig. 2(b). Note that the oscillations are fast, i.e., $\Omega \gg T_2^{-1}$.

Figure 3 shows the solution at the same limit of $T_2=2T_1$ as a function of the small-signal absorption $\alpha_0 L/\delta^2$, for $t_r=0.01$. It can be seen that there is a minimum value of absorption over which the instability occurs. The lower line describes the onset of instability as we increase the intensity, while the upper line describes the same as we decrease it. The existence of an upper limit to the instability range is due to the saturation in this system.

Figure 4 describes the solutions at the limit of rapid collisional dephasing, as a function of t_r for the case of $T_2=0.2T_1$. Here we find a family of distinct solutions; each of them extends over a certain length range. Note that these solutions are found in relatively long interaction lengths. The oscillation frequency is much smaller than in the previous case and is of the order of T_1^{-1}. It is inversely proportional to the interaction length. The threshold intensity is much below the saturation intensity, and again we observe the existence of upper and lower bounds.

V. DISCUSSION

In our study of instabilities of counterpropagating waves in a Kerr medium[2] we showed that it can be fully explained as parametric oscillations in a distributed feedback (DFB) formed by the phase grating in the medium. We interpret the instability as a beating between the input fields and the sidebands, generated by the nonlinear interaction, through a gain-feedback process. Figure 5 shows schematically the two input fields at ω, each with two sidebands oscillating at $\omega\pm\Omega$. The sidebands are identified by the corresponding terms of Eq. (15).

We now apply this model to the two-level system. Let us first consider the feedback mechanism. It is clear that the standing-wave pattern formed by the counterpropagating waves modulates both the absorption and the index of refraction. The grating which is formed supplies feedback

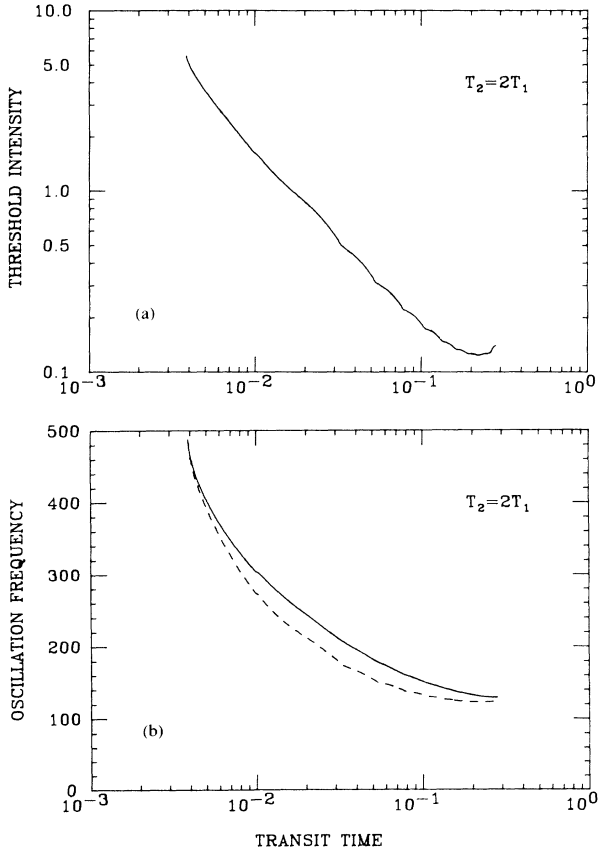

FIG. 2. Threshold intensity (a) and oscillation frequency (b) as a function of the transit time in the medium, for pure radiative broadening, $T_2=2T_1$, where $\delta=100$ and $\alpha_0 L/\delta^2=0.1$. In Figs. 2–4 the intensity is expressed in units of the saturation intensity at δ, the frequency is the angular oscillation frequency, in units of T_2^{-1}, and the transit time is in units of T_2. The dashed line in (b) is the generalized Rabi frequency which corresponds to the peak field values, taken from (a).

for fields with frequencies close to those of the input fields. This feedback decreases as the field frequencies are detuned away from the input frequency. Such distributed feedback structure has modes similar to those of mirror resonators.[10]

Which of these modes will be excited first is determined by the gain at these frequencies. The interaction between a strong pump and a weak probe of different frequencies in a TLA was first studied by Mollow.[11] It was found that the strong pump may induce gain or loss to the weak probe. The peak of the gain, in the limit of pure radiative broadening, occurs when the probe frequency is shifted from the pump by approximately the generalized Rabi frequency

$$\Omega_g = \left[\left(\frac{\delta}{T_2} \right)^2 + \kappa^2 E^2 \right]^{1/2} . \tag{21}$$

It is reasonable to expect then, that if enough feedback is given, self-oscillations at that frequency would occur. The first resonance of the distributed resonator is located $\sim 1/t_r$ from the Bragg frequency ω_0. The conditions for self-oscillations are optimal if the resonance condition and gain peak coincide, i.e.,

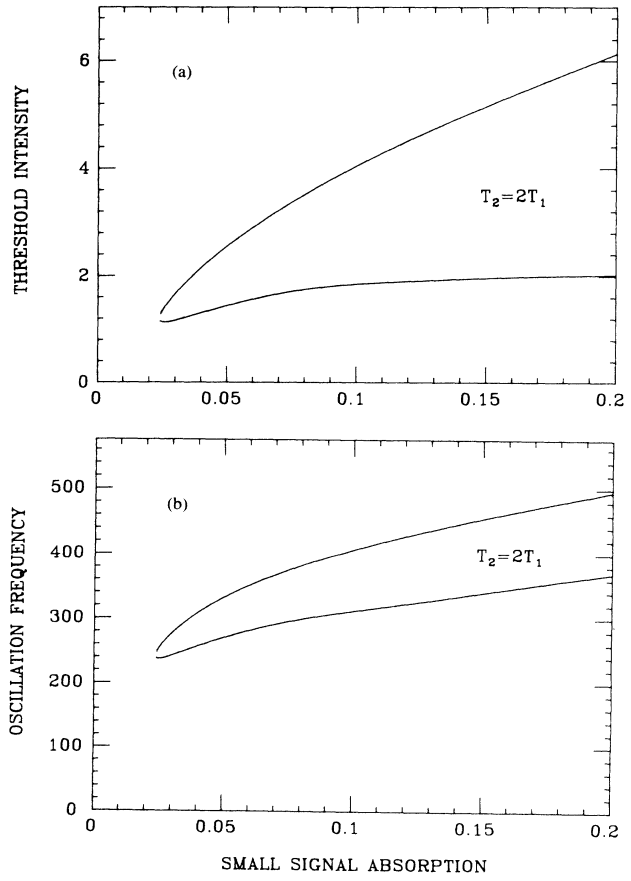

FIG. 3. Threshold intensity (a) and oscillation frequency (b) as a function of the small-signal absorption $\alpha_0 L/\delta^2$, in the medium, for pure radiative broadening, $T_2=2T_1$, where $\delta=100$ and $t_r=0.01$.

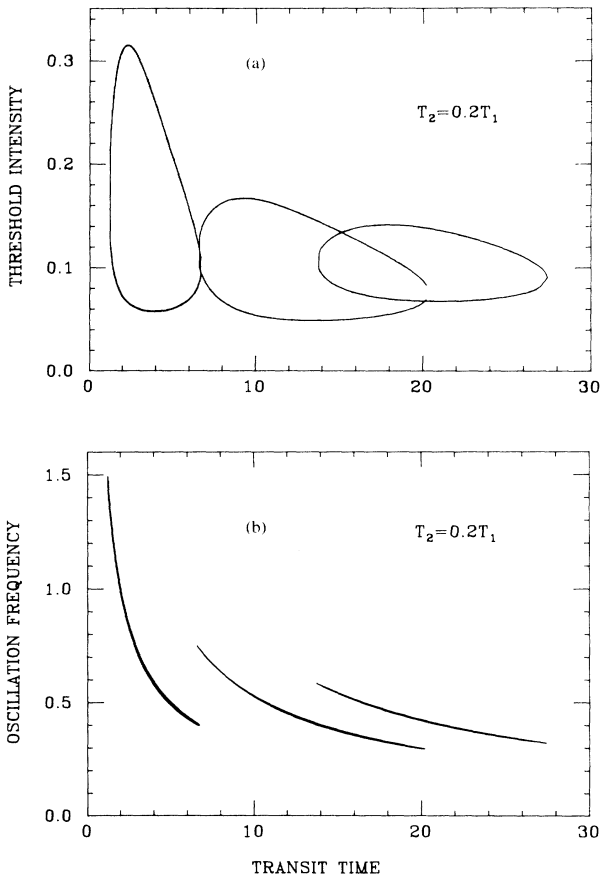

FIG. 4. Threshold intensity (a) and oscillation frequency (b) as a function of the transit time in the medium, for rapid collisional dephasing, $T_2=0.2T_1$, where $\delta=100$ and $\alpha_0 L/\delta^2=0.25$.

$$\Omega \sim \Omega_g \ , \qquad \Omega \sim \frac{1}{t_r} \ . \tag{22}$$

Thus, there is an optimal interaction length for the oscillations to occur, which is given for a low intensity by $t_r/T_2 \sim 1/\delta$. Since we assumed large detuning values, i.e., $\delta \gg 1$, it follows that $\Omega_g T_2 \gg 1$, and we conclude that Rabi oscillation would occur in a short medium, namely, when $t_r/T_2 \ll 1$. The results of the stability analysis, shown in Fig. 2, indeed confirm this behavior. The dashed line in Fig. 2(b) depicts the generalized Rabi frequency, corresponding to the peak field values as taken

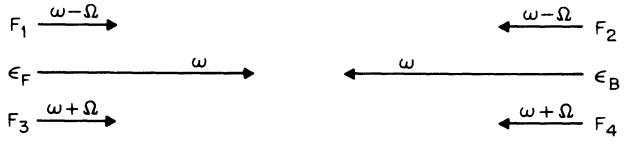

FIG. 5. Two counterpropagating input beams ε_F and ε_B, with their excited sidebands, $F_1(\omega-\Omega)$, $F_2(\omega-\Omega)$, $F_3(\omega+\Omega)$, and $F_4(\omega+\Omega)$.

from Fig. 2(a).

Let us now proceed to discuss the limit of rapid collisional dephasing. Figure 6 depicts the gain for a probe beam as a function of its detuning from the pump, for $T_2=0.2T_1$. In Fig. 6(a) we chose the pump intensity to be $0.1I_s$, of the order of the threshold intensity found in the stability analysis of this limit (Fig. 4). It can be clearly seen that the peak of the gain is approximately at T_1^{-1}, and there is no net gain at the Rabi frequency. Only when we increase the pump intensity significantly [Fig. 6(b)], does the gain at the Rabi frequency appear, and at higher intensity [Fig. 6(c)] exceed that of the T_1^{-1}. In order for oscillations to be built at T_1^{-1}, there should be enough feedback at that frequency. This suggests that such oscillation would appear in a medium where $t_r \sim T_1$. Indeed, we find T_1^{-1} oscillations in a relatively long medium and low threshold intensities. Moreover, we can identify the different solution curves of Fig. 4 as modes of the DFB resonator. This behavior is completely analogous to that found in a Kerr medium. This should not surprise us since it is well known that in this limit a TLA can be modeled by a Kerr medium with a response time T_1.

An interesting point is the phase-matching question. It is clear that at low powers the sidebands of the forward propagating field are not coupled to those of the backward propagating field due to phase mismatch. For example, the waves F_1 and F_3 of Fig. 5 are coupled through the nonlinear interaction with ε_F, since the copropagation geometry ensures perfect phase matching. However, the waves F_1 and F_4 are not coupled due to the fact that phase matching is not possible in a counterpropagating geometry. At high intensities, the strong nonlinear dispersion shifts the phase of all waves, and the coupling between F_1 and F_4 becomes phase matched.

Let us consider now the feasibility for experimental observation of these instabilities. In the above analysis we concentrated on a homogeneously broadened medium. Although an experiment in atomic beams can be imagined, it is more practical to consider an experiment in a Doppler-broadened medium. The effect of Doppler broadening is not as harmful as it may look at first sight. It is clear that only the zero velocity atoms contribute to the feedback mechanism, and hence in a simplified picture we may assume that the interaction is only with them. The other atoms may generate gain or loss. If the fields are detuned to one extreme of the Doppler line, their absorption would be small, but they would still contribute to gain at the sideband frequency. It is therefore expected that Doppler broadening will not alter the predicted behavior significantly.

Generation of sidebands at the Rabi frequency was already demonstrated by Harter *et al.* in a single beam experiment.[12] The gain for these frequencies is so large that spontaneous generation can occur. The contribution of the feedback given by the counterpropagating

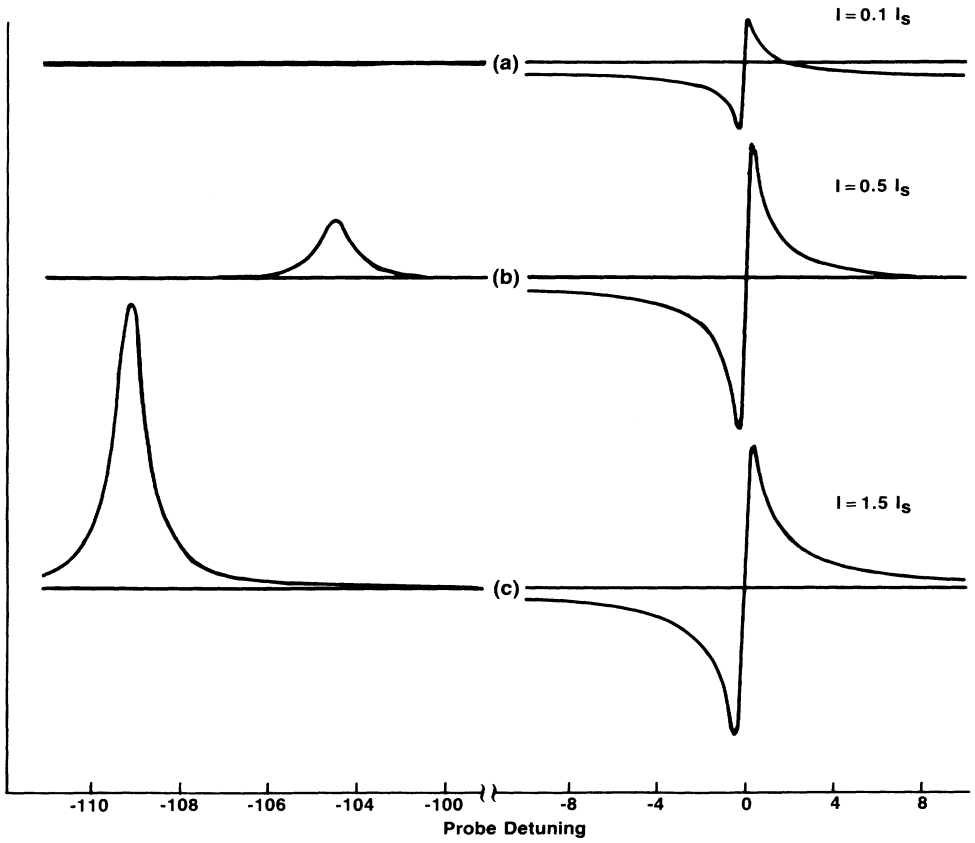

FIG. 6. The gain for a probe beam as a function of its detuning from the pump, for $T_2=0.2T_2$, and for three pump intensities (a) $0.1I_s$, (b) $0.5I_s$, and (c) $1.5I_s$. The gain at large detuning is at the generalized Rabi frequency, while the gain and loss at small detunings are approximately at $\pm T_1^{-1}$.

beam is just to lower the threshold. However, we predict that in a long medium and low intensities, population pulsations at T_1^{-1} can be induced and observed. Consider, for example, sodium vapor where $T_1=16$ nsec and $I_s=10$ mW/cm^2. In order to observe experimentally the T_1 oscillation shown in Fig. 4 we should set T_2 to 3 nsec in a cell about 2 m long. The threshold intensity is predicted to be of the order of 60 W/cm^2. The laser should be detuned 5 GHz from the line center, and the absorption at the laser frequency should be adjusted to about 0.25.

In conclusion, we have studied the stability of the interaction of two counterpropagating waves in a two-level medium, and showed that it exhibits a rich spectrum of self-oscillations. We have explicitly shown the behavior at two limits: one of pure radiative broadening and the other of rapid collisional dephasing. However, it should be noted that other solutions, at the intermediate range of T_2, exist and show complicated behavior, which is not always understood. We believe that an experiment in a two-level medium, which would demonstrate the occurrence of T_1^{-1} oscillations, is feasible.

ACKNOWLEDGMENTS

We wish to acknowledge discussions with A. A. Friesem and Y. Prior. Part of this work was performed at the Weizmann Institute of Science, Israel.

APPENDIX

The solutions of the linearized Bloch equations are

$$d_{+=}=-D_0\frac{(\Phi_1+\Phi_3^*)X_0^*X_++(\Phi_3+\Phi_2^*)X_0X_-^*}{X_0X_0^*(\Phi_1+\Phi_2^*)+2\frac{T_2}{T_1}+2\lambda T_2}\ , \tag{A1}$$

$$d_-=d_+^*\ ,$$

$$s_+=i\Phi_1(X_0d_++X_+D_0)\ ,$$

$$s_-^*=-i\Phi_2^*(X_0^*d_++X_-^*D_0)\ .$$

The matrix $\mathbf{M}_2$ of Eq. (18) is

$$\mathbf{M}_2=\begin{bmatrix}0&0&M_{1,3}&M_{1,4}\\0&0&M_{2,3}&M_{2,4}\\M_{3,1}&M_{3,2}&0&0\\M_{4,1}&M_{4,2}&0&0\end{bmatrix}\ , \tag{A2}$$

where

$$M_{1,3}=\Phi_1(Y_1Z_2+Z_4)-(\Lambda-i\theta)\ ,$$

$$M_{1,4}=-\Phi_2Y_2Z_2\ ,$$

$$M_{2,3}=-\Phi_2^*Y_1Z_2\ ,$$

$$M_{2,4}=\Phi_2^*(Y_2Z_2+Z_4)-(\Lambda+i\theta)\ ,$$

$$M_{3,1}=\Phi_1(Y_1Z_1-Z_3)-(\Lambda-i\theta)\ ,$$

$$M_{3,2}=\Phi_1Y_2Z_1\ ,$$

$$M_{4,1}=\Phi_2^*Y_1Z_1\ ,$$

$$M_{4,2}=\Phi_2^*(Y_2Z_1-Z_3)-(\Lambda+i\theta)\ .$$

The following is a list of notations:

$$\Lambda=\lambda T_2t_r=\lambda L/c\ ,$$

$$\Phi_1=(1-i\delta+\lambda T_2)^{-1}\ ,$$

$$\Phi_2=(1-i\delta+\lambda^*T_2)^{-1}\ ,$$

$$\Phi_3=(1-i\delta)^{-1}\ ,$$

$$\tilde{\Omega}_0=\kappa T_2\sqrt{I}\ ,$$

$$X_i=\kappa T_2\varepsilon_i,\quad i=0,+,-$$

$$a=\lambda T_2+T_2/T_1+\tilde{\Omega}_0^2(\Phi_1+\Phi_2^*)\ ,$$

$$b=\tilde{\Omega}_0^2(\Phi_1+\Phi_2^*)\ ,$$

$$c=T_2/T_1+\tilde{\Omega}_0^2(\Phi_3+\Phi_3^*)\ ,$$

$$d=\tilde{\Omega}_0^2(\Phi_3+\Phi_3^*)\ ,$$

$$Y_1=\alpha_0L\frac{T_2}{T_1}\tilde{\Omega}_0^2(\Phi_1+\Phi_3^*)\ ,$$

$$Y_2=\alpha_0L\frac{T_2}{T_1}\tilde{\Omega}_0^2(\Phi_2^*+\Phi_3)$$

$$Z_1=\frac{1}{bc-ad}\left[-\left[\frac{a-b}{a+b}\right]^{1/2}\left[1+\frac{(a^2-b^2)^{1/2}-a}{b}\right]+\left[\frac{c-d}{c+d}\right]^{1/2}\left[1+\frac{(c^2-d^2)^{1/2}-c}{d}\right]\right]\ ,$$

$$Z_2=-\frac{1}{bc-ad}\left[\left[\frac{a-b}{a+b}\right]^{1/2}\left[1+\frac{(a^2-b^2)^{1/2}-a}{b}\right]+\left[\frac{c-d}{c+d}\right]^{1/2}\left[1+\frac{(c^2-d^2)^{1/2}-c}{d}\right]\right]\ ,$$

$$Z_3=\alpha_0L\frac{T_2}{T_1}\frac{1}{(c^2-d^2)^{1/2}}\left[1+\frac{(c^2-d^2)^{1/2}-c}{d}\right]\ ,$$

$$Z_4=\alpha_0L\frac{T_2}{T_1}\frac{1}{(c^2-d^2)^{1/2}}\left[-1+\frac{(c^2-d^2)^{1/2}-c}{d}\right]\ .$$

[1] *Instabilities in Active Optical Media*, edited by N. B. Abraham, L. A. Lugiato, and L. M. Narducci [J. Opt. Soc. Am. B **2** (1985)].

[2] *Optical Instabilities*, edited by R. W. Boyd, M. G. Raymer, and L. M. Narducci (Cambridge University Press, Cambridge, 1986).

[3] Y. Silberberg and I. Bar-Joseph, Phys. Rev. Lett. **48**, 1541 (1982).

[4] Y. Silberberg and I. Bar-Joseph, J. Opt. Soc. Am. B **1**, 662 (1984).

[5] A. L. Gaeta, R. W. Boyd, J. A. Ackerhalt and P. W. Milonni, Phys. Rev. Lett. **58**, 2432 (1987).

[6]P. Mandel and G. P. Agrawal, Opt. Commun. **42**, 269 (1982).
[7]F. L. Lippi, J. R. Tredicce, N. B. Abraham, and F. T. Arecchi, Opt. Commun. **53**, 129 (1985).
[8]L. Allen and J. H. Eberly, *Optical Resonance and Two-Level Atoms* (Wiley, New York, 1975).
[9]H. J. Carmichael, Opt. Acta **27**, 147 (1980).
[10]H. Kogelnik and C. V. Shank, J. Appl. Phys. **43**, 2327 (1972).
[11]B. R. Mollow, Phys. Rev. A **5**, 2217 (1972).
[12]D. J. Harter and R. W. Boyd, Phys. Rev. A **29**, 739 (1984).